Mesoscopic noise studies of atomic motions in cold amorphous conductors

G. A. Garfunkel*, G. B. Alers, and M. B. Weissman
Department of Physics, University of Illinois at Urbana-Champaign, 1110 West Green Street, Urbana, Illinois 61801
(Received 11 September 1989)

The dynamics of slow low-energy atomic motions in the amorphous conductors C-Cu and Si-Au were probed using conductance fluctuations in nanometer-scale samples in the temperature range 4–30 K. Ample evidence was found of isolated fluctuators with both tunneling and thermally activated kinetics, with the estimated density of sites at 4 K close to that expected from the anomalous heat capacity of amorphous solids. However, a detailed statistical analysis revealed that the conductance-fluctuation data were inconsistent with a picture of independent randomly fluctuating two-level systems. Direct evidence of non-two-state behavior was occasionally seen in discrete switching in the voltage traces. It was also found that anneals up to 100 K were usually sufficient to randomize features in the spectral density. The statistical analyses and the strong sensitivity to relatively weak anneals suggest that intersite interactions are prevalent in these systems.

INTRODUCTION

In 1971 Zeller and Pohl[1] published data on the low-temperature thermal properties of a variety of amorphous materials. The heat capacity for $T<1$ K was found to be approximately linear in T, in excess of the T^3 dependence expected and observed in crystalline materials, and the thermal conductivity was found to scale approximately as T^2 instead of the expected T^3. Since the publication of this data, extensive investigations on a broad range of amorphous systems have revealed anomalous behavior in the acoustic, dielectric, and optical properties, and other thermal properties, and have shown that some of the anomalies appear to be universal features of amorphous solids, including both insulators and conductors measured in the superconducting regime.[2,3] Early on it was proposed that some aspects of the anomalies could be understood at a phenomenological level in terms of collections of so-called "two-level systems" (TLS).[4] These were two-level excitations or modes which were proposed to exist in excess of the thermal phonons. The unmistakable distinctions between amorphous and crystalline solids and the apparent quantitative universality of certain features of amorphous solids have inspired extensive work on amorphous materials. Despite limited success in describing some aspects of two specific systems,[5,6] there is no firm understanding of the general nature of the low-temperature excitations at the microscopic level. The approximate universality of the density of states and of the strain coupling of the low-temperature excitations are somewhat puzzling. Within the context of the TLS picture, it is even more surprising that a product of the density of states, the strain coupling, and an elastic constant, which determines the ratio of a phonon mean free path to its wavelength, has a much more nearly universal value than do the factors taken separately.[7] This universality raises the suspicion that the density of states is itself limited by interactions between sites due to the same strain coupling responsible for the interaction with phonons and that the resulting coupled excitations might be qualitatively different from TLS. However, no numerically consistent version of such a theory has yet been developed.

The occupation of the low-energy modes will, of course, fluctuate in equilibrium with kinetics determined by interactions with the phonon bath, electron bath, or possibly with other modes. These fluctuations must occur whether or not the modes have a two-level character. These equilibrium occupation fluctuations, or a subset of them, are a likely cause of the $1/f$ noise found in disordered materials.[8] The prevalence of universal-conductance-fluctuation multiple-scattering terms[9,10] prevents the noise signal from diminishing with decreasing temperature despite the presumed freezing out of the fluctuators. Such universal-conductance-fluctuation noise in disordered conductors is expected to be a rather nonspecific probe of any fluctuations in strength or position of scatterers.[9]

By studying the noise in extremely small volume samples, one has a unique opportunity to study the kinetics and other properties of individual or small groups of fluctuators. While, in typical noise samples, the effects of isolated fluctuators are obscured by all the other fluctuators, resulting in a Gaussian signal,[8,11] in sufficiently small nanometer-scale samples the effects become apparent. The kinetics of the individual fluctuators will be manifest in features or bumpiness in the noise spectral density,[8] in certain statistical properties which characterize the noise,[8,12,13] and in direct observation of discrete conductance jumps.[14–16]

Mesoscopic noise techniques have proved quite useful in characterizing fluctuating sites in several amorphous and crystalline materials.[8,12–16] Some materials in some temperature ranges do exhibit mainly two-state switching, while others show more complicated patterns indicating significant interactions between the fluctuating sites. However, no previous studies have dealt with noise from miscellaneous atomic motions (as opposed to special

subsets involving changes of charge state) in an amorphous material near the regime in which TLS are believed to be important in the main thermal properties.

In this paper we report on such studies performed on extremely small-volume samples of C-Cu and Si-Au in the temperature range of 4–30 K. (A brief account of the highlights of the results has appeared previously.[17]) Ample evidence was found of spectral features exhibiting both thermally activated and weakly temperature-dependent, presumably tunneling, kinetics. The observation of features represents the first evidence of isolated fluctuators in amorphous metals, although individual switching sites have been seen in the less thoroughly amorphous metal sputtered Bi. The estimated density of fluctuators is in good agreement with the estimates based on heat-capacity measurements of typical amorphous materials.[2,3]

Although we shall see that the temperature dependence of the noise spectra below 30 K could be analyzed in terms of double-well systems, we shall also see that more complicated constructs, perhaps involving interactions between double-well systems, are required to fully describe various statistical parameters of the noise. In particular, in some instances, individual switching states which were not double-well systems were directly observed.

The terms "fluctuator" and "mode" are used interchangeably in this report. When possible, we analyze the data in terms of double-well systems. Reference is occasionally made to a TLS, which describes the behavior of a double-well system in the low-temperature limit. However, it is understood that the modes active below 1 K, the standard TLS regime, are not necessarily the same as those in the 4–30 K regime studied.

EXPERIMENTAL CONSIDERATIONS

Noise measurements were made on five C-Cu and two Si-Au small-volume samples, and a number of comparatively large-volume control samples. All small-volume samples except C-Cu No. 5 were fabricated using a new "double-step-edge" nanolithography technique which requires only conventional optical lithography equipment.[18] The technique allows for the fabrication of small wires with triangular cross sections, configured as true four-probe resistors suitable for noise studies. The effective noise volumes for the double-step-edge samples were in the range of 1×10^{-16} cm^3, with effective diameters of 30–40 nm and lengths of 100–200 nm. C-Cu No. 5 had dimensions of ~1 μm$\times$(40 nm)^2 and was fabricated by means similar to the usual single-step-edge technique.[19] With the exception of C-Cu No. 3, which was close to the metal-insulator transition, all samples were metallic with essentially temperature-independent conductivities below 50 K. Both the C-Cu and Si-Au films were prepared by rf magnetron sputtering from compound targets into room-temperature sapphire and glass substrates. The films were quite stable with respect to high-temperature anneals (30 min at 90 °C) and to thermal cycling. Noise magnitudes on large-volume samples were always reproducible to within 10% after thermal cycling between 4 and 300 K. As-deposited and annealed films were examined by high-resolution scanning-tunneling electron microscopy (STEM), including microprobe x-ray analysis, and by sputtered neutral mass spectroscopy. They were almost entirely amorphous, although small crystalline inclusions of the metallic component (1.5–2.0 nm for Cu, 1.0 nm for Au) occupied up to about 2% of the volume of the films. No significant difference was seen in the STEM studies for the as-deposited and annealed films.

Noise data were usually taken with a dc bridge arrangement, using PAR 113, 117, or 185 amplifiers for front-end amplification. The noise signal was filtered with eight-pole Butterworth low-pass anti-alias filters, and digitized to 12-bit resolution. Fast Fourier transforms (FFT's) were performed on a SKYMNK array processor, and power spectra and various statistical parameters were automatically computed and stored using a Digital Equipment Corporation (DEC)LSI11/23 host microcomputer. Data were continuously monitored, and any anomalous sweeps, due to power glitches, etc., were automatically rejected by the acquisition program. Interfering narrow-band pickup (e.g., 60 Hz) was subtracted from the power spectra, allowing for a relatively accurate determination of the spectral slope. Measurements were done with current densities of $(1-2)\times10^4$ A/cm^2, and the normalized noise-magnitude parameter of the small-volume samples was typically within a factor of 4 of the values determined on the large-volume control samples.

SPECTRAL FEATURES

Spectral features [i.e., deviations from simple power-law behavior of the resistance fluctuation spectral density $P(f)$] are usually the most accessible indicator of small sample-size effects.[8] Noise spectra in double-step-edge samples of C-Cu and Si-Au were always featureless from room temperature down to approximately 30–40 K. At lower temperatures, spectral features were almost always apparent. This is what we expect if, upon lowering T, the average number of active fluctuators decreases to roughly less than about one per octave.[12] A representative plot of spectral features found at low T is shown in Fig. 1 for C-Cu No. 1. The data clearly show a diminishing of the spectral features with increasing temperatures. At 16 K the spectrum is very close to pure power-law behavior with no apparent features. Electrical transients caused irreversible changes in the spectrum after the lowest two temperature runs, so only the four spectra above 5 K are reversible samplings of the same feature.

Several features were successfully tracked in both Si-Au and C-Cu over a limited temperature range. Figure 2 shows relatively clean, reproducible data on a feature found in C-Cu No. 1 between 9.5 and 12.3 K. A plot of the peak frequency versus T^{-1} for this data is shown in Fig. 3. The data show a good fit to the expected Arrhenius form for thermally activated behavior, $f_{\text{peak}}=f_0e^{-E'/kT}$, where f_{peak} frequency, E' is the activation energy, and f_0 is the attempt rate. We find $E'\approx15\pm1$ meV and $f_0\approx5\times10^8$ Hz (uncertain to about a factor of 3).

The temperature dependence of the peak amplitude

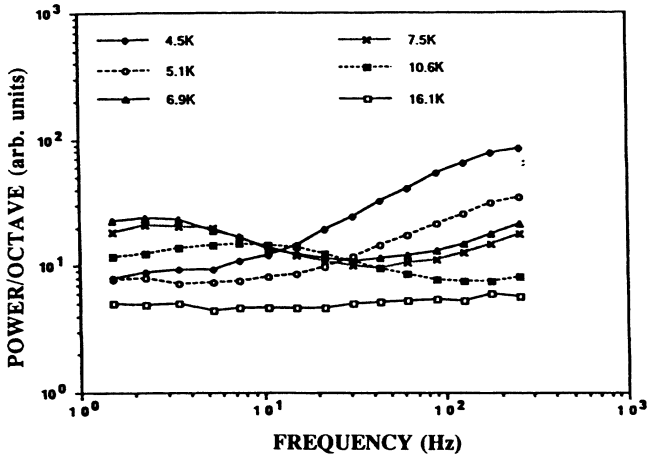

FIG. 1. Noise spectra, expressed as power per octave in arbitrary but fixed units, are shown at six temperatures for sample C-Cu No. 1. Changes among the four highest temperatures were reversible, but small electrical transients caused irreversible changes at the two lowest temperatures.

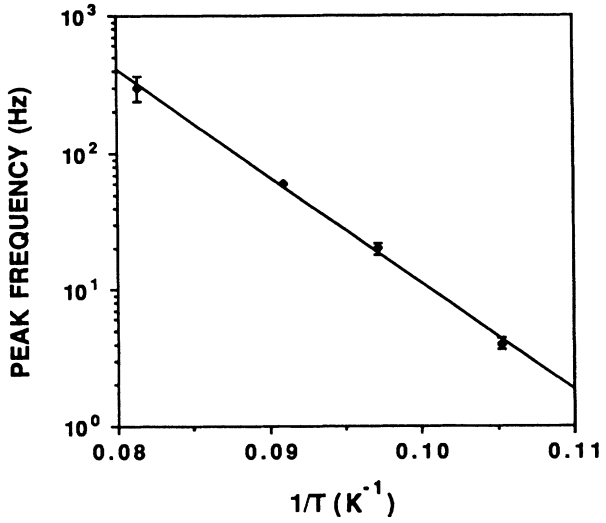

FIG. 3. The peak frequency vs inverse temperature from the data of Fig. 2 is shown. The relative positions of the peaks are obtained by fitting displaced copies of the spectra at pairs of temperatures (e.g., 9.5 and 10.3 K) to each other, and checking the shift in the log frequency scale. The resulting frequency shifts are substantially more accurate than would be obtained by estimating peak frequencies independently for each spectrum.

yields some information on energy splitting E between the two eigenstates. In this case the peak amplitude is only weakly temperature dependent. The contribution from the duty cycle (cf. Appendix B) to the temperature exponent of the peak amplitude is

$$\partial \ln[\mathrm{sech}^2(E/2kT)]/\partial \ln T = (E/kT)\tanh(E/2kT) ,$$

(Ref. 8) or $\sim(E/kT)$ when $kT \ll E$ and $\sim E^2/2(kT)^2$ for $E \ll kT$. Thus, although according to universal conductance fluctuation theory[9,10] for any particular atomic motion, the squared effect on the conductance should decrease with T, roughly as T^{-2}, for any given fluctuator the noise magnitude can increase as an arbitrarily large power of T (locally), in the regime $kT \ll E$. The slight increase in the peak amplitude with increasing T seen in

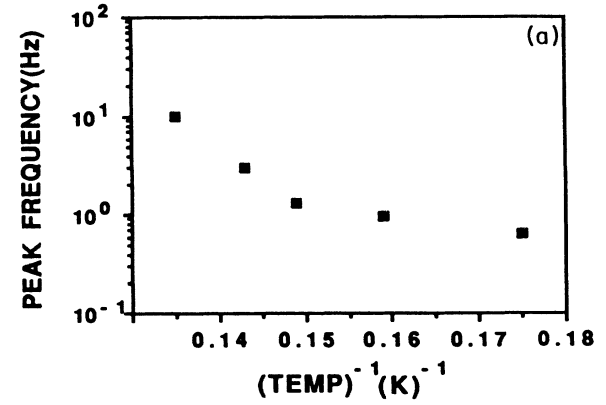

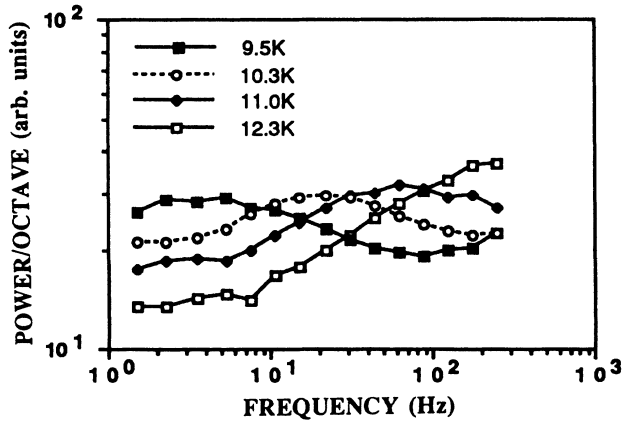

FIG. 2. Noise spectra for sample C-Cu No. 1 on a different cool down from those shown in Fig. 1 are shown, on the same scale as in Fig. 1.

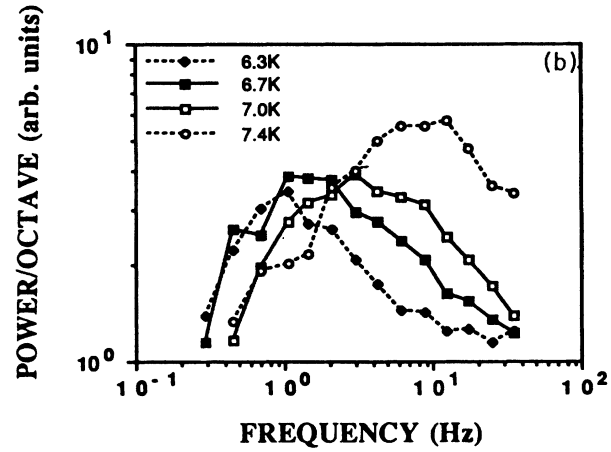

FIG. 4. (a) The dependence of the peak frequency on inverse temperature is shown, obtained from (b) noise spectra for sample Si-Au No. 1, using the fitting procedure described for Fig. 3.

Fig. 2, while partially obscured by the background spectrum, implies that for this fluctuator $kT \approx E$ for $T \approx 10$ K.

Other examples of the temperature dependence of features are given in Figs. 4 and 5. The feature shown in Fig. 4 for Si-Au exhibits a strong deviation from the Arrhenius form, clearly indicating nonactivated behavior over part of the temperature range. The knee at 6.7 K in the plot of peak frequency versus T^{-1} may signify a transition from nonactivated behavior below 6.7 K to activated behavior above 6.7 K. Fits to an Arrhenius form for the top three data points yield $E' = 12$ meV and $f_0 = 3 \times 10^9$ Hz. The features of Fig. 5 clearly fail to fit the Arrhenius form. Tunneling kinetics via single-phonon processes for TLS's will show peak frequencies f_{peak} proportional to $\coth(E/2kT)$ (Ref. 20) with exponents

$$\partial \ln(f_{\text{peak}})/\partial \ln T = (E/2kT) \times \operatorname{sech}(E/2kT) \times \operatorname{csch}(E/2kT)$$

ranging from 0 for $2kT \ll E$ up to 1 for $2kT \gg E$. Note that the data in Fig. 5(b) show tunneling-type behavior at the relatively high temperatures of 20–33 K. With the possible exception of Fig. 5(c), the observed exponents of about 1 are consistent with the expected behavior for single-phonon tunneling in this temperature range. Overall, the observation of spectral features with both thermally activated and tunneling kinetics is consistent with the expected extrapolated behavior of TLS. This, of course, does not preclude other possible models, but the observation of isolated spectral features at least means that some sort of fixed modes with discrete relaxation rates are present.

The low attempt rate found for the activated transitions is worth noting, since it may indicate relatively large fluctuating objects, with either small vibration frequencies or negative activation entropies. On the other hand, the existence of at least one fluctuator with nonactivated, apparently tunneling kinetics up to 30 K suggests that some fluctuators may have low masses or narrow tunneling barriers. At any rate, the individual features show a diversity which would not be evident in the aggregate behavior.

The next obvious question is whether these modes are present in about the right concentration to account for typical amorphous heat capacities. The density of fluctuators was estimated from the size of variations in the spectral density (cf. Appendix A). It was found that annealing to temperatures of only 60–100 K was usually sufficient to scramble the random features in the spectral density, and thus the distribution of active fluctuators.

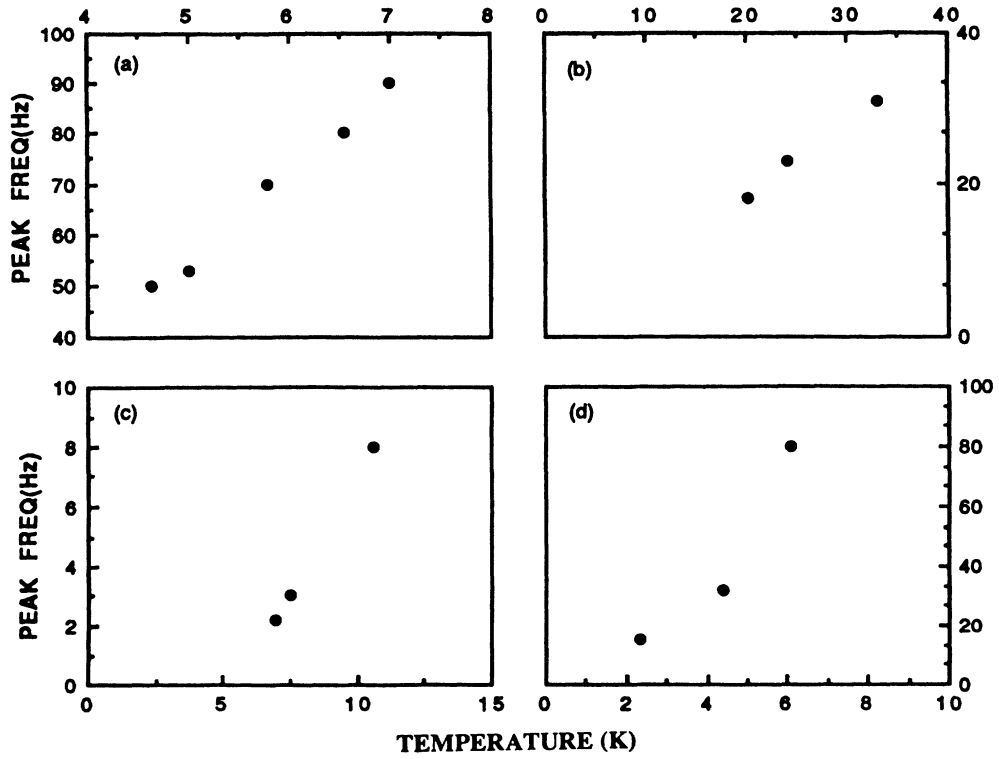

FIG. 5. Peak frequencies vs temperature are shown for several cool downs of two samples. (a), (b), and (c) are from C-Cu No. 1. (d) is from C-Cu No. 2. The relative frequency shifts are accurate to about 15%.

New random distributions of fluctuators, and effectively new samples, could thus be obtained by repeated anneals at moderate temperatures. The density was determined via Eq. (A4) and measurements of the frequency exponent $\gamma \equiv -\partial \ln P(f)/\partial \ln f$. For C-Cu No. 5 with the relatively large volume of 10^{-15} cm^3, the exponent γ was measured at 4.2 K after each of five consecutive anneals. The variance in γ is a reliable indicator of random variations, since it has almost no systematic variation with any sample properties, including annealing, about the average value of 0.98 in C-Cu at 4.2 K. The band used for the γ determination consisted of three adjacent octaves, just below 60 Hz. This was sufficient to give enough precision without including a large enough bandwidth to significantly reduce the γ fluctuations through averaging. The standard deviation of γ was 0.04 (with error limits determined by statistics, as discussed in Appendix A), and from this the density of Lorentzians per factor of e duty cycle (i.e., per kT in level spacing) and per factor of e in frequency was estimated to be 1.5×10^{16}/cm^3 within a factor of 3. Here the error range allows for about a 10% chance each for the true value to be above or below the estimated range, using a Bayesian estimator as discussed in Appendix A. Assuming fluctuators are distributed over 12 decades in frequency ($\sim$28 factors of e), the total density of fluctuators would then be 1×10^{17}/cm^3 K. The estimate is good to about a factor of 5, due to additional uncertainties in the frequency extrapolation. Comparable values for the total density were estimated for the other samples, all of which had volumes about an order of magnitude smaller. The value of 1×10^{17}/cm^3 K from C-Cu No. 5 is most reliable, however, due to difficulties in estimating the volumes of these smaller samples. The densities are in reasonable agreement with the density of TLS of about 3×10^{17}/cm^3 K (with a range of more than a factor of 3 each way) estimated from the extrapolated heat capacity of amorphous insulators[2] or superconducting amorphous metals.[3]

DISCRETE SWITCHING

Occasionally discrete switching was visible in the voltage traces on top of the continuous background noise signal. Such observations, though not as common as spectral features, obviously provide the most compelling evidence of the nature of at least some of the low-energy excitations. Clearly distinguishable switching was seen in eight runs on both C-Cu and Si-Au. Except on one run, it was found to be stable provided the sample was not annealed or subjected to transients. The fractional conductance jumps were in the range of 0.1–1 %. Significant uncertainties in the lead resistance and sample length prevented a reliable estimate of the magnitude of the conductance jumps per phase coherent region. Assuming phase coherence lengths of 10 nm, the estimated change in conductance per phase coherent region ranged from $0.1-0.2e^2/h$ in C-Cu to $10\ e^2/h$ in Si-Au, with an uncertainty of a factor of 10. In addition, the observed conductance jumps are necessarily the largest ones, though the approximate agreement between the noise power levels of the small- and large-volume samples implies that the conductance jumps were not more than a few times the average.

Low-duty cycle switching was observed most often, as expected in standard TLS models for which far more states have asymmetries greater than kT (low-duty cycle) than less than kT (high-duty cycle).

Selected traces of high-duty cycle switching observed in Si-Au are shown in Fig. 6. A total of 40 traces were recorded, 20 of which are shown here. Approximately one-third of the selected traces, or $\sim$15% of all traces,

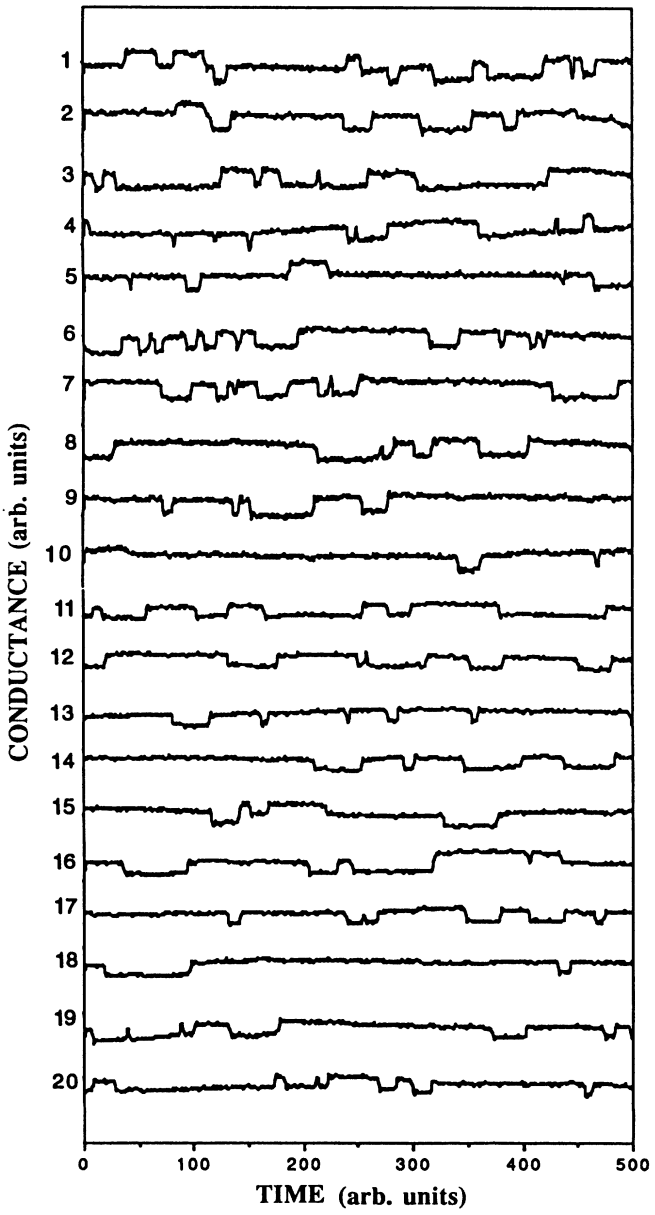

FIG. 6. Selected sweeps of resistance vs time are shown for Si-Au No. 1 at 5.5 K. Each sweep represents 500 data samples, with a sampling time of 2.6 ms. The vertical displacements of the sweeps are for viewing clarity. The steps represent a fractional conductance change of about 0.5%.

can easily be seen to be pathological compared to that expected for an independent TLS. The first, second, fourth, fifth, fifteenth, and sixteenth traces, for example, exhibit switching between three conductance states, not two states. Since switching was seen relatively infrequently, during about 5% of all runs on all samples (looking in a two decade frequency band), the odds are very low, 0.25%, that two independent TLS would be observed simultaneously. More important, however, is the observation in traces 15 and 16 of direct transitions between the lowest (voltage) level and the highest level. Direct transitions might be expected for a three-level system, but, of course, would be highly improbable for the case of two independent TLS. The argument applies whether or not the fluctuators are close enough that universal conductance fluctuation interference terms might cause one to modulate the conductance change of the other.

Apart from the traces which showed signs of three-state switching, a few two-conductance-state switchers displayed non-Markovian kinetics indicating that two physical states are not sufficient to completely describe the system. The sixth and eighteenth traces can be seen to switch with either duty cycles or characteristic frequencies that are improbable. Also, note that while most traces only exhibit two-level switching, most of those that show three-level switching, in fact, have multiple transitions into the third (high) state. Though the limited number of sweeps imposes significant sampling errors, a histogram of the lifetimes revealed a larger than expected tail on the distribution of "up" states at high lifetime values (sweeps containing three-level switching were omitted from the histogram). All of these properties differ from those of a fixed two-state system. They cannot be modeled with a three-state system either.

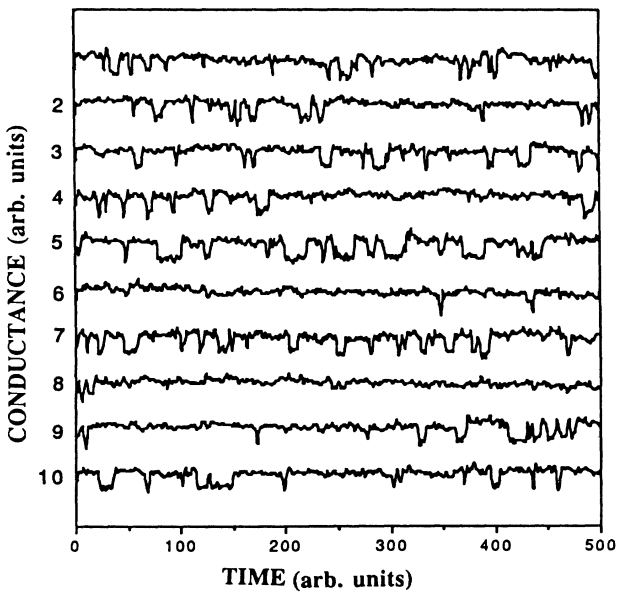

FIG. 7. Selected sweeps of resistance vs time are shown for C-Cu No. 4 at 4.3 K. Each sweep represents 500 data samples, with a sampling time of 1.3 ms. The vertical displacements of the sweeps are for viewing clarity. The steps represent a fractional conductance change of about 0.3%.

The most dramatic examples of kinetics differing from a two-state Markov process are shown in Fig. 7 for sweeps recorded in one of the C-Cu samples at 4.3 K. Extensive switching is apparent in the fifth and seventh traces while the fluctuator is essentially inactive in the sixth and eighth traces. Such behavior could arise from two interacting TLS in which one modulates the duty cycle of the other, or in a three-state system. The fluctuations lasted for over an hour, and then abruptly stopped. The sample was not subject to any transients, electrical or thermal, and for these reasons, it is not known whether these dramatically non-Markovian fluctuations were typical of "equilibrium" properties or not.

NOISE VARIANCE

In most cool downs, analyzable discrete switching was not found. Even when it was present, simple inspection is not generally a very sensitive way of analyzing its statistical properties. We have developed a set of statistical characterization techniques for noise which are entirely automated and suitable for use whether or not discrete steps are detected. An understanding of the statistical techniques, which have been discussed in a series of earlier articles,[8,12,13] is essential to the interpretation of most of the data, in which discrete switching was not apparent or not easily analyzable. The techniques employed here are reviewed in Appendix B. The noise in both C-Cu and Si-Au was found to be Gaussian within the sensitivity of the measurements from intermediate temperatures of $\sim 100-200$ K down to ~ 30 K, below which non-Gaussian effects were usually apparent. At room temperature the noise was always featureless but frequently non-Gaussian. The variance, obtained from a series of Fourier transforms, in the measured spectral density in the ith octave c_i normalized to the value for Gaussian noise (see Appendix B) occasionally showed weakly non-Gaussian values of $\sim 1.1-1.4$ even in large-volume Si-Au samples of $\sim 10^{-12}$ cm^3 at room temperature, and are most likely associated with the same mechanism giving rise to the dramatic increase in the noise magnitude above $T \sim 150$ T shown in Fig. 8. Some rather large-scale rearrangements would be required to account for the large-sample non-Gaussianity. We did not study this high-temperature range in any detail.

It should be noted that for one of the samples, which was close to the metal-insulator transition, artifacts of universal conductance fluctuation coupling[9] could result in non-Gaussian behavior from low-frequency modulations of the *amplitude* of fluctuators that would not be indicative of deviations from TLS behavior. On the other hand, modulations of the *duty cycle* or *characteristic frequency* of fluctuators can only be associated with actual deviations of the fluctuating structure from a simple two-state model. All samples but one were relatively metallic. Thus, the non-Gaussian effects observed in the metallic samples were not artifacts of the universal conductance fluctuation coupling. The normalized variances c_i exhibited a range of values and functional forms in the

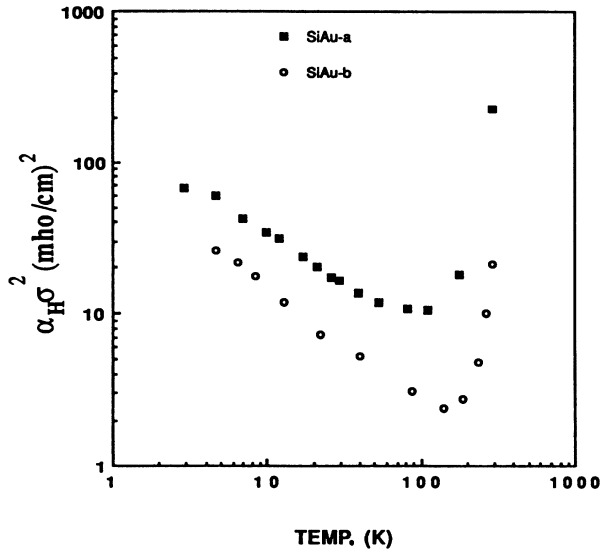

FIG. 8. The conductance noise power spectral density, averaged over four octaves near 20 Hz, is shown for two Si-Au samples.

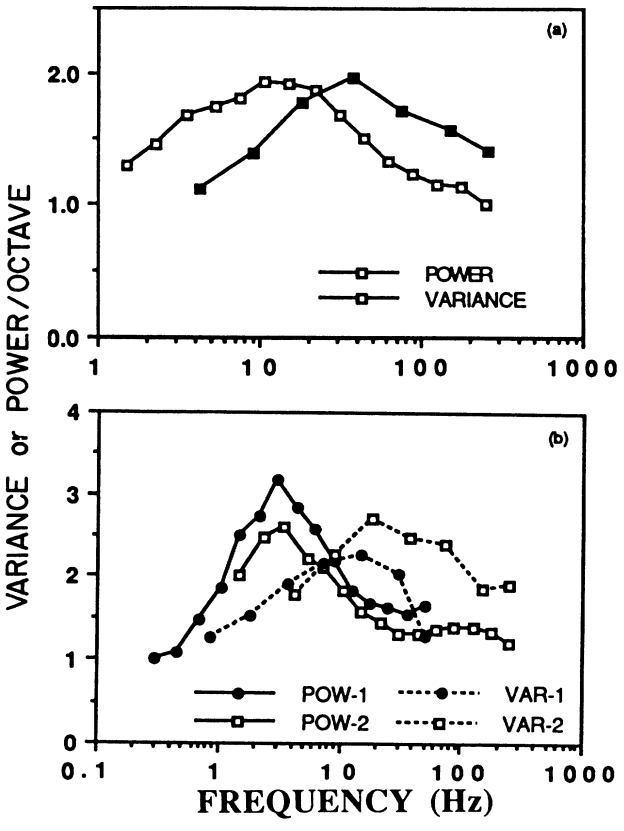

FIG. 9. (a) The noise power (in arbitrary units) and the normalized variance are shown for sample C-Cu No. 3 at 4.3 K. (b) Similar data are shown for the same sample on a different cool down. The two sets were taken before and after a small switching transient.

4–30 K regime. An example of classical behavior of the variance for a two-state fluctuator is shown in Fig. 9. In Fig. 9(a) the variance c_i is seen to peak approximately two octaves above the peak in the power, as expected whenever the background is Gaussian and equal to, or larger than, the magnitude of the presumed two-state Lorentzian component.

Many examples of this type of behavior were recorded. For the data presented in Fig. 9(b), and in some other runs, two-state switching was visible in the voltages traces. Assuming the duty cycle is not too small, this is usually a sufficient, though not necessary, condition for the observation of non-Gaussian variances. In many cases switching is not perceptible. Figure 10 shows a relatively clean feature with weak but measurable excess variance, for which no switching was observed. As discussed in Appendix B, the high-duty-cycle fluctuators have smaller variances than low-duty-cycle fluctuators with the same power levels. (Here, by high-duty cycle, we mean close to 50% occupation of each state; low-duty cycle means that either the high or low state is rarely occupied.) Thus, the low variances combined with the relatively strong feature in the spectral density imply one, or a few, fluctuators with high-duty cycles. The variances in Fig. 11 were computed on a signal exhibiting low-duty-cycle, low-frequency switching. The low number of accumulated sweeps accounts for the large scatter in the data. While the feature is only about twice as large as that in Fig. 10, the variances are dramatically larger and appear to increase monotonically with frequency. This type of behavior is consistent with the low-duty-cycle, low-

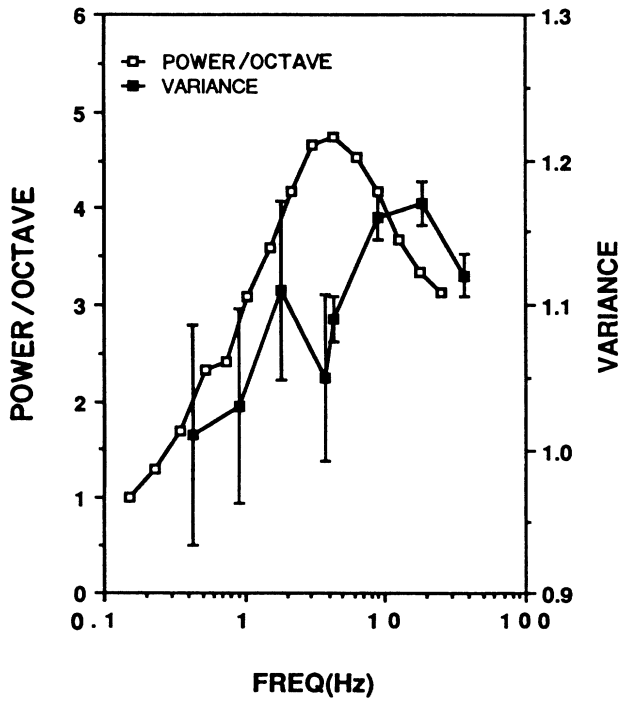

FIG. 10. Noise power per octave and normalized variance are shown for C-Cu No. 1 at 5.3 K.

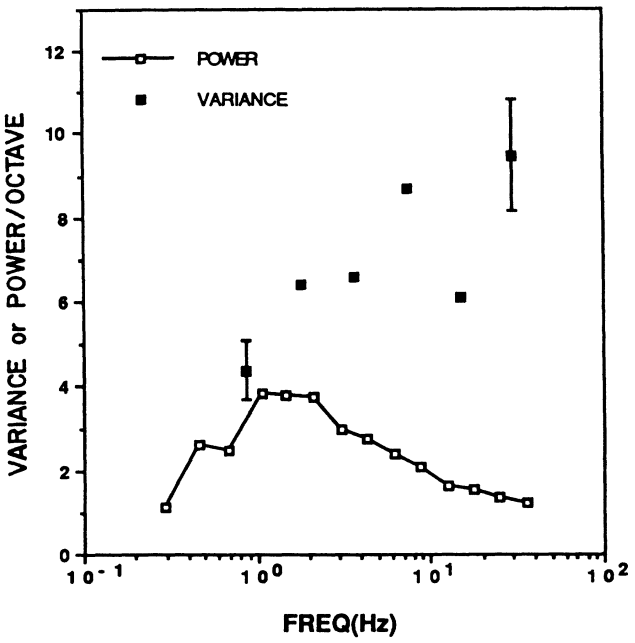

FIG. 11. Noise power per octave and normalized variance are shown for Si-Au No. 1 at 6.7 K.

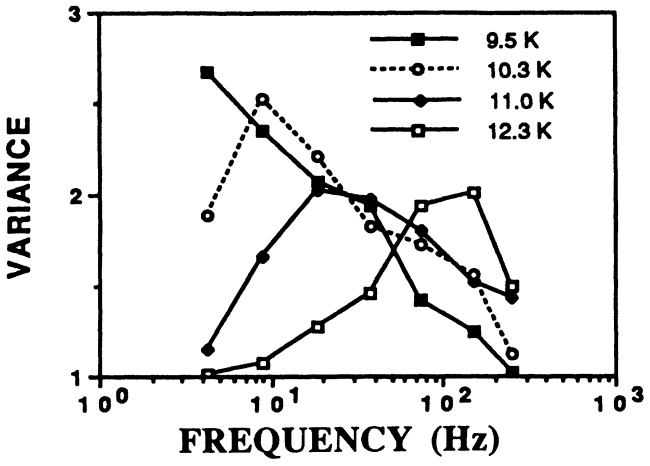

FIG. 12. The variances are shown for the data whose power spectra appear in Fig. 2.

background limit. Assuming that this feature comes from a two-state switcher, from the ratio of the feature to the background, the variance should peak about 4 ± 1 octaves above the peak in the power, around the top frequency measured. This holds regardless of the duty cycle.

In one instance the variance data was clearly inconsistent with the expected c_i for a two-state switcher. We shall examine this case in some detail because it illustrates the surprising amount of information available in the various fourth-order statistical properties. Figure 12 gives the variances as a function of temperature for the spectral densities given in Fig. 2. The observed variance peaks approximately one octave *below* the peak in the power, and is thus not consistent with the usual model of two-state switching with a Gaussian $1/f$ background. The peak in the variance consistently tracked the power peak over the whole measured temperature range. Low amplitude, barely discernable switching was noted, with a very low-duty cycle of 1 ± 1 event per sweep. The location of the peak in the variance is a very weak function of the frequency exponent of the background spectrum, whose precise value cannot possibly account for the observed shift. It is highly unlikely that components in the background could be the source of the excess variance, since the feature in the spectrum and the peak in the variance are so well correlated over the whole temperature range. The data could be accounted for, however, in terms of a system more complicated than a simple two-state switcher.

We consider a limited class of modulated two-state systems consisting of objects whose characteristic rates and/or fluctuation amplitudes themselves fluctuate. The object in question could not be produced simply by allowing the overall step size to fluctuate, since that would produce maximum variance at the peak of the spectrum. Likewise, fluctuations in the overall rate, produced by barrier-height fluctuations, could not account for the data. These would simply shift a fixed spectral power around, giving negative correlations between the power fluctuations in different octaves, but such negative correlations were not observed. Fluctuations in only the faster of the two characteristic rates, in the limit of low-duty cycles, would not produce any fluctuations in the noise power at frequencies much above the characteristic frequency, since the effects due to the fluctuating duty cycle and due to the fluctuating characteristic frequency would cancel in that range. In fact, one can show analytically that for such a model, the peak in the variance occurs a factor of $3^{1/2}$ lower in frequency than the peak in the power, for small variations of the fast rate. Since we could not devise any other simple models which were consistent with the covariance matrices and power spectra and their strongly correlated temperature dependence, we believe that a model in which only the faster of the two rates for a switcher fluctuates, probably approximately describes this unusual case. A small, very low-duty-cycle switcher was barely observable in these runs.

In summary, a range of functional forms of c_i were observed. Most of the range is consistent with the broad distribution of duty cycles, conductance step sizes, and characteristic rates expected for two-state systems in glasses giving universal conductance fluctuation noise. In one instance, however, the spectrum of the variance was not consistent with that expected for independent two-level switching. We could only account for this behavior in terms of a fluctuator, one of which characteristic relaxation rates itself fluctuated.

SECOND SPECTRA

Second spectra were acquired on most of the samples. We will be primarily interested in the frequency dependence of the second spectra, which reflects the temporal dependence of the excess (non-Gaussian) power fluctua-

tions (cf. Appendix B). For noise with normalized variances close to unity, the second spectra were white noise as expected. Independent or random two-level switching should also have approximately white-noise second spectra, regardless of the variance. An example of this classical behavior for independent switching is shown in Fig. 13 for data from Si-Au at 10.5 K. The second spectra are given for each of the top seven octaves of the power spectrum. The spectra are plotted in terms of the power *per unit frequency,* so white-noise spectra appear flat, and the magnitude is normalized to unity for Gaussian noise for each octave. The limited number of second-order sweeps accounts for substantial sampling error in the lowest second-order octaves. The data was smoothed by nearest-neighbor averaging. These second spectra confirm the presence of at least some fluctuators that behave as noninteracting TLS, at least on the time scale of the measurement.

Of the data that showed significant excess variance, however, a majority (six of seven) had non-white-noise second spectra. Second spectra computed from 13 second-order sweeps from C-Cu at 5.3 K are shown in Fig. 14. No switching was evident in the voltage traces, and the variances were relatively small, reaching a maximum of 1.29 in octave 9 and remaining less than 1.2 in all other octaves. Strong low-frequency components are seen to dominate the second spectra for octaves 8, 9, and 10. The low-frequency components of the second spectra are not a result of linear drift in the power, as the power was stable throughout all 13 sweeps. After subtraction of the white-noise component, the excess non-white-noise component is found to scale as $f^{-1.2}-f^{-1.3}$ for octaves 9 and 10. The excess second spectra can be interpreted as the spectral density of some variable which modulates the noise power. In terms of a TLS picture, the results indicate that TLS are subject to low-frequency interactions. The second spectra measured on the signal showing strong switching in Fig. 9 is given in Fig. 15. The non-white-noise component is similar to that in Fig. 14, and the magnitudes of the white-noise and the non-white-noise components clearly peak in the same octaves. In this case it is obvious that the power and excess variance are completely dominated by the switching, and the non-white-noise component must be associated with anomalous switching of the fluctuator. The essential point is

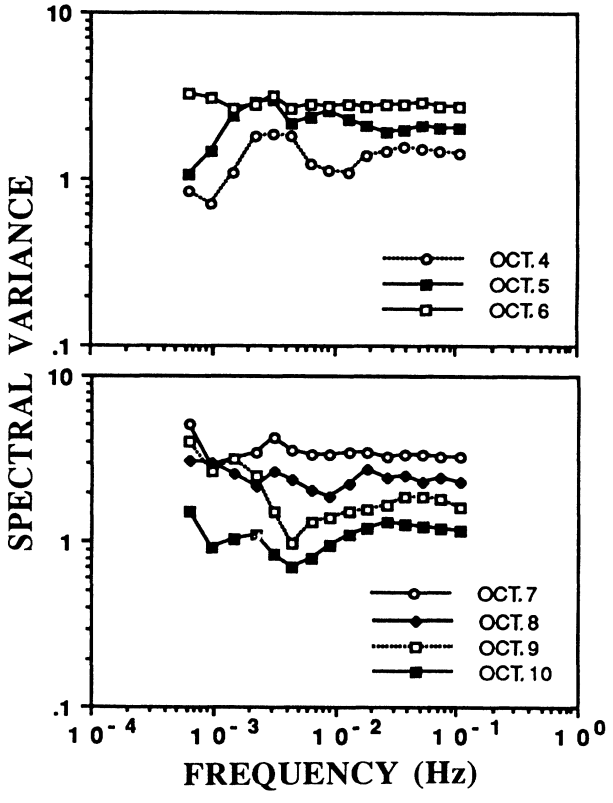

FIG. 13. Second spectra are shown for sample Si-Au No. 2 at 10.5 K. Each spectrum is normalized to unity for Gaussian noise. Spectra are taken from the top seven octaves of the first spectrum, which was acquired at a sampling rate of about 390 Hz. Statistical errors range from about ±60% for the lowest second-order octave to about ±6% for the highest second-order octave. Data are smoothed by nearest-neighbor averaging.

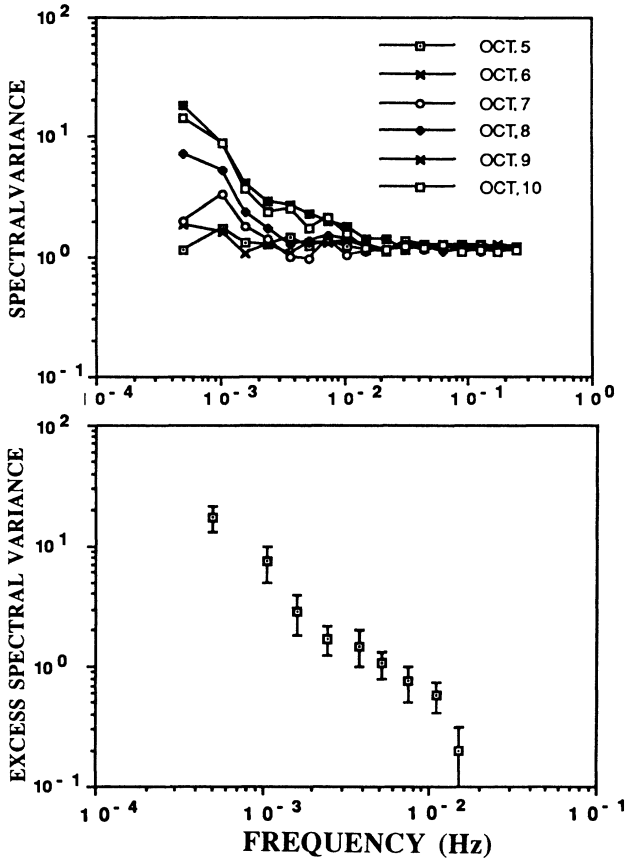

FIG. 14. Normalized second spectra are shown for sample C-Cu No. 1 at 5.3 K. Data were taken at a sampling rate of 852 Hz. (b) The non-white-noise component of the second spectrum of octave 9 is shown, obtained by subtracting the average of the top three second-order octaves. The best power-law fit is $f^{-1.2}$. A similar plot, best fit with $f^{-1.3}$, is obtained from octave 10.

that the second spectra reveals such behavior regardless of whether switching is visible in the voltage traces.

We consider another case in which it is possible to analyze the data, and the nature of the modulations, in more detail. Figure 16 shows the second spectra computed from two second-order sweeps on Si-Au at 7.4 K. The spectra are white noise at high frequencies, and scale more like $1/f$ to $1/f^2$ at low frequencies. Examples of the voltage traces are given in Fig. 17. Direct inspection of the second-order sweeps, given in Fig. 18, reveal that at least in this case the low-frequency components are continuous and nonmonotonic fluctuations, and likely to be associated with the same fluctuating degree(s) of freedom responsible for the large white-noise component. The average spectral densities and variances from each of the two second-order sweeps are shown in Fig. 19.

The data are roughly consistent with that expected for a non-Gaussian fluctuator with a relatively Gaussian background. The powers and the variances of each of the two sweeps, however, are seen to differ by a non-negligible amount. On the basis of this data and the cor-

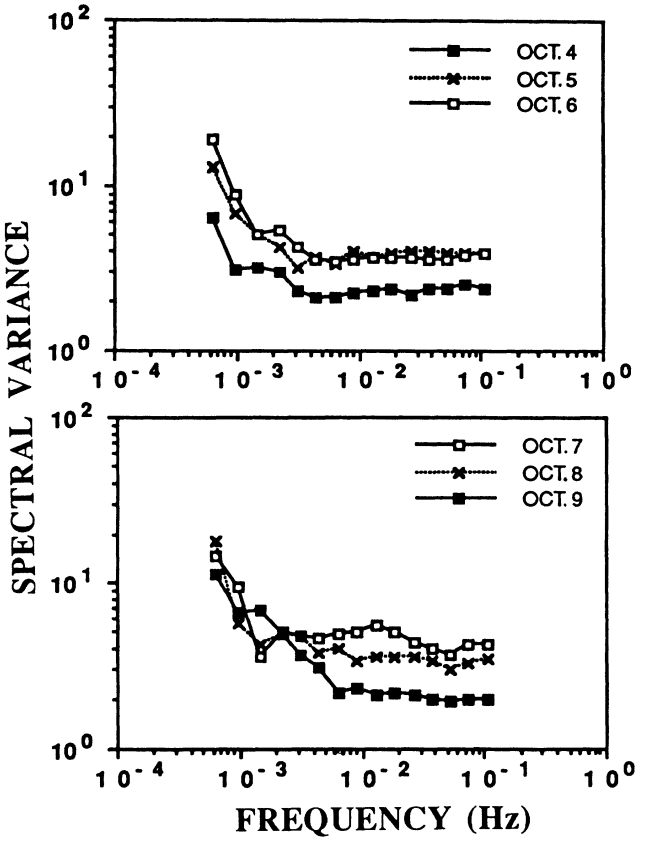

FIG. 16. Second spectra are shown from Si-Au No. 1 at 7.4 K, with a sampling rate of about 390 Hz. Uncertainties are similar to those of Fig. 13.

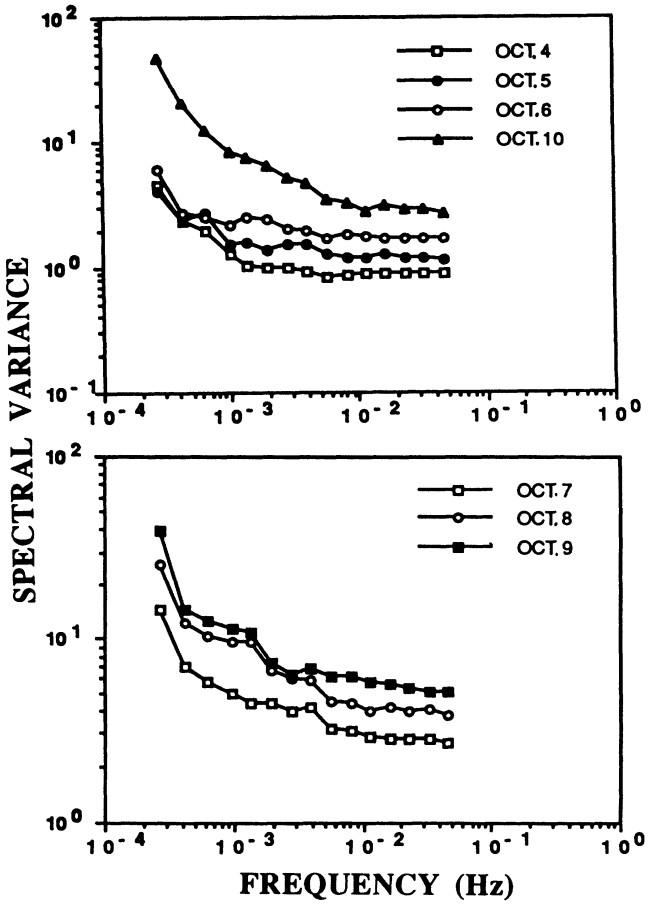

FIG. 15. Second spectra from sample Si-Au No. 1 at 5.5 K, sampling rate 169 Hz, are shown. The data are the same as in Fig. 11. Uncertainties are about 50% for the lowest second-order octaves and about 5% for the highest.

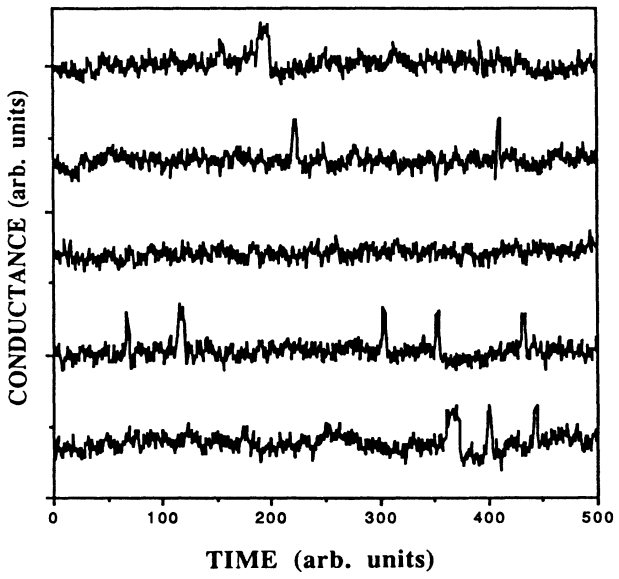

FIG. 17. The resistance vs time sweeps for Si-Au No. 1 are shown, for the same data as in Fig. 16.

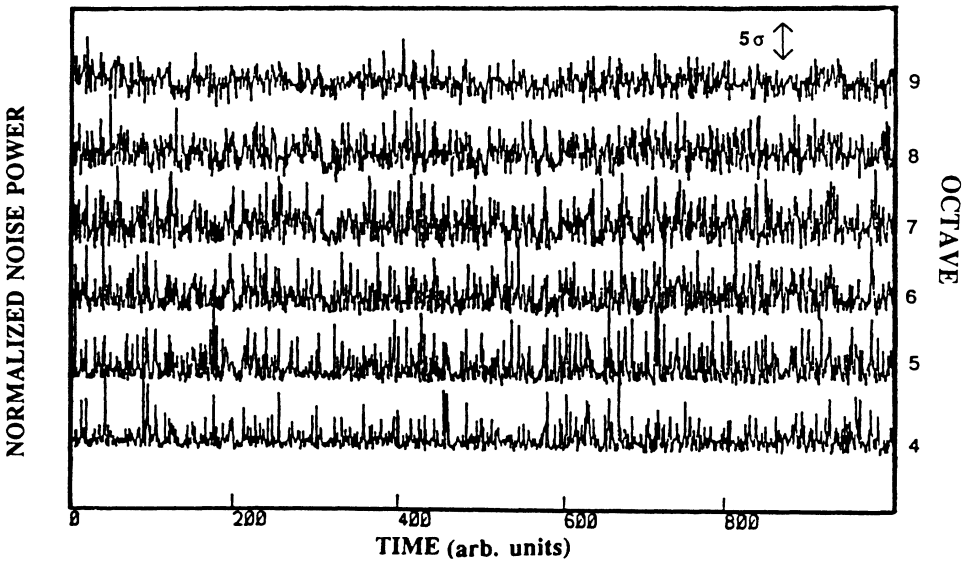

FIG. 18. Second-order sweeps are shown for the same data as in Figs. 16 and 17. Sweeps show the noise power in each of octaves 4–9 as a function of time. Each octave is normalized so that its Gaussian variance fits the scale shown. Vertical displacements are for viewing only. The time for each second-order data point was about 2.6 s, so each second-order sweep here represents about 45 min of data.

responding second spectra, it can be shown that the large low-frequency components of the second spectra are associated with slow fluctuations in the *duty cycle* of the fluctuator, and not its amplitude. Note first that in Fig. 19

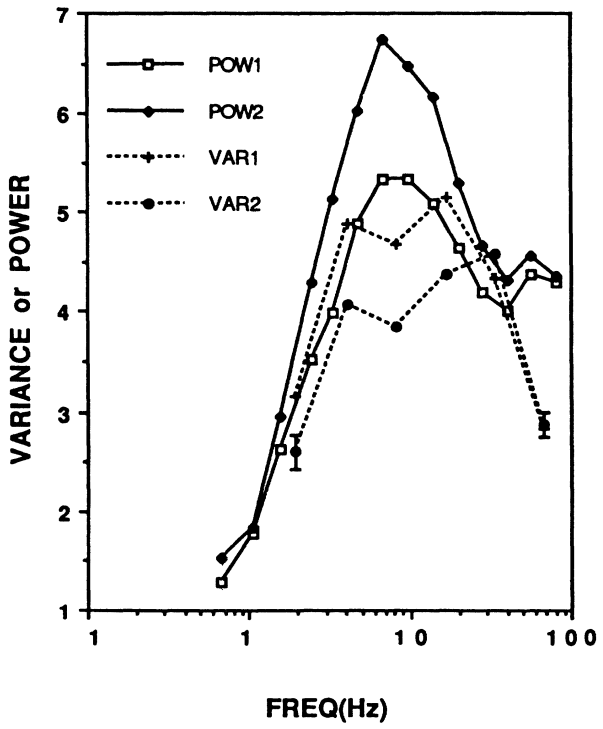

FIG. 19. Both the noise power per octave and the normalized variance are shown for the same conditions as in Figs. 16–18. The two data sets are from two consecutive second-order sweeps.

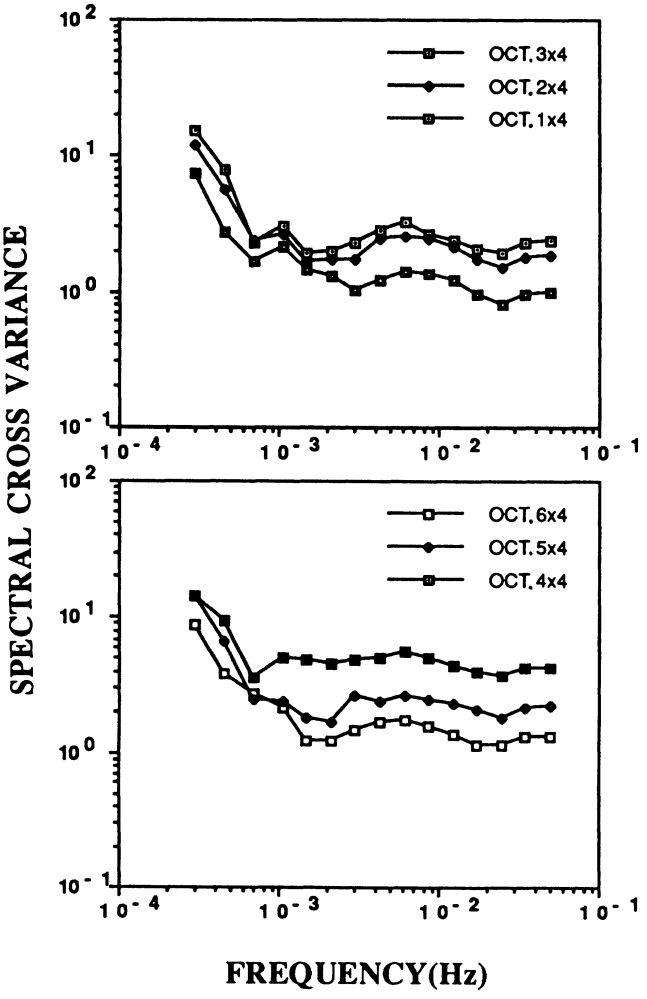

FIG. 20. Several second-order cross spectra are shown from the data used in the preceding figures.

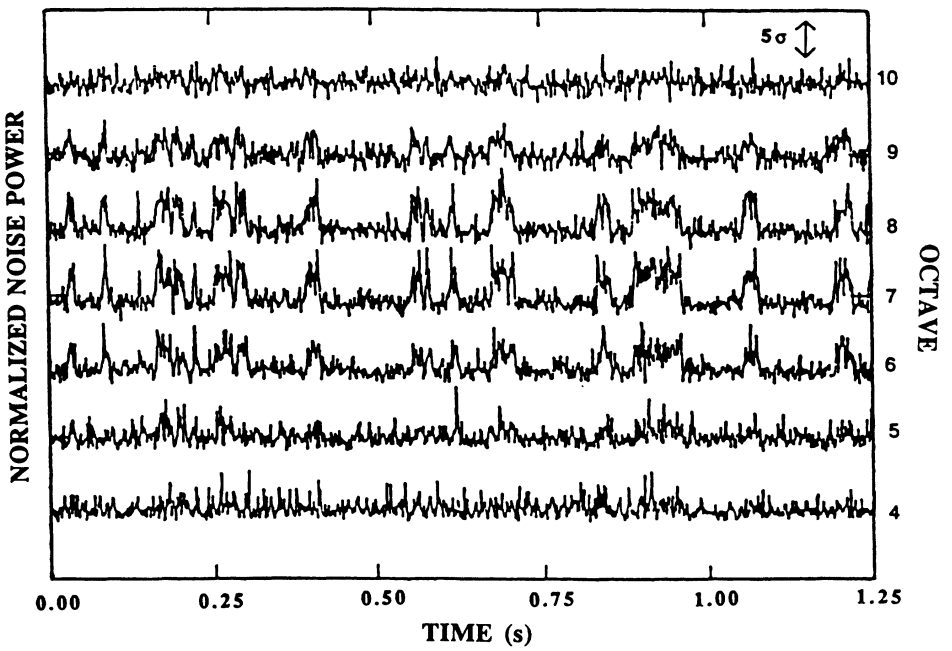

FIG. 21. Second-order sweeps exhibiting switching, from C-Cu No. 1 at 16.1 K, with a data sampling rate of 852 Hz. The same normalization is used as in Fig. 18.

the sweep with greater power exhibited lower variances. This is what we would expect if the duty cycle was larger, on the average during the lower variance sweep. In fact, the change in the variance might be even more pronounced if the effects of the background could be suppressed. The change in the peak power of $\sim 50\%$ (after subtracting the background) is roughly consistent with the change in variance, if the duty cycle changes from an average of two events to three events per sweep.

If, on the other hand, the amplitude of the switches had changed instead of the duty cycle, we would expect the variance to remain constant since amplitude factors are divided out in the normalization for c_i. In the presence of a Gaussian background, we would, in fact, expect the variance to increase with increasing power, not decrease as observed. Thus, it is the duty cycle and not the amplitude that is fluctuating. It might be argued that drifts in the amplitude are dominating the variance, and that the drifts were simply stronger during the second sweep than the first. This possibility can be ruled out since the second spectra of the second sweep shows slightly smaller low-frequency components than the first sweep. Note that if the characteristic frequency of the fluctuator was changing as opposed to the duty cycle, then the non-white-noise components of the second-order cross spectra (between octaves on opposite sides of the peak in the power) would be strictly negative. These cross terms shown in Fig. 20 are positive, hence, fluctuations in the rate can also be ruled out. Unlike the anomalous variance discussed earlier, this site can be explained by fluctuations in the slower, not the faster, of the two characteristic rates for a small duty-cycle switcher.

In summary, the difference in the characteristics of the noise between the two second-order sweeps is consistent with a change in the duty cycle of the fluctuator, and not its amplitude or rate. This implies that the non-white-noise low-frequency components of the second spectra are associated with changes in the thermodynamics of the fluctuator. The universal conductance fluctuation modulation or interaction effects, would manifest themselves as amplitude fluctuations, and can thus be ruled out.

Modulations in the duty cycle (or frequency) could only be associated with structural changes. Had the raw data been available, a direct analysis of the switching might have lead to the same conclusion. The significance of the analysis technique employed above is that it may be used even when switching is not evident, as in Fig. 14, or when other types of non-Gaussian effects are present. An example of this case is given below.

During one run in C-Cu at 16 K, dramatic effects were observed in the second-order sweeps and spectra. Discrete switching was seen in the *second-order sweeps*. A typical second-order sweep is given in Fig. 21. Ten such sweeps were accumulated over a period of 8 h. The switching was very stable, with all sweeps looking essentially identical to those shown, and persisted until the sample was reannealed. No switching was evident in the first-order sweeps, and the spectral density, given as the 16 K data in Fig. 1, was almost featureless. From the magnitude of the second-order switching it can also be determined that the rms voltage fluctuations, while in the "up" state, were $\sim 15\%$ above those in the "down" state. The second spectra for this data is shown in Fig. 22. After subtracting the Gaussian contribution of unity from the second spectra, this "excess second spectra" is seen to have approximately a Lorentzian form, as one

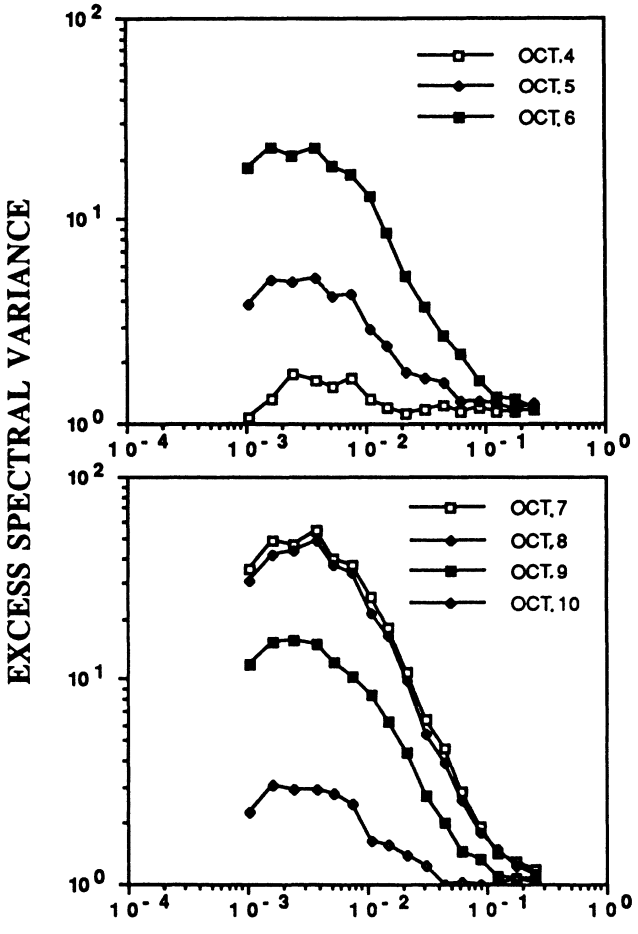

FIG. 22. Second spectra are shown for the data shown in Fig. 21.

would expect for random two-state switching. This scaling can also be seen in the second-order cross spectrum given in Fig. 23, where the Gaussian contribution inherently averages to zero. The observed switching can be modeled most simply in terms of a three-level system. For example, the system may fluctuate relatively quickly between two higher-energy states, but sit dormant a majority of the time in the third lowest-energy state.

Anomalous behavior was also seen in second spectra acquired in sample C-Cu No. 3. Representative second spectra and the corresponding spectral density and c_i are given in Figs. 24 and 25. The variances are relatively low, and Gaussian contribution has been subtracted from the second spectra to emphasize the frequency dependence of the non-Gaussian part. Unlike the previous data, the second spectra here show a range of behavior. Octaves 6 and 7 appear nearly Gaussian in the top half of the second spectrum, and weakly non-Gaussian in the lower half. Octaves 4 and 5 have relatively clean frequency independent excess second spectra, while octaves 8, 9, and 10 display inverse-power scaling closer to $1/f$ over a comparatively broad range. The data is consistent with one fluctuator acting as an independent TLS, at or below octave 4, and a separate fluctuator with a $\sim 1/f$ second spectra, centered around octaves 9 and 10. The background noise, which dominates in octaves 6 and 7 intermediate between the two fluctuators, is nearly Gaussian. Some structure is apparent in the second spectra of octaves 8, 9 and 10 at around 10 mHz. The postulated low-frequency fluctuator cannot be associated with this structure, as octave 4 corresponds to ~ 2 Hz.

Non-white-noise second spectra may occur for reasons independent of the fluctuator dynamics. Two closely spaced fluctuators may have independent kinetics yet "interact" electronically in the sense that the conductance switching δG due to one fluctuator depends on the configuration of another. Aside from the usual universal conductance fluctuation interaction[9] which applies to all defects within a dephasing length L_i of each other, another interaction mechanism exists in samples close to the metal-insulator transition. For such samples, current paths are very inhomogeneous on the scale of L_i, and a fluctuating TLS may induce large fluctuations in the

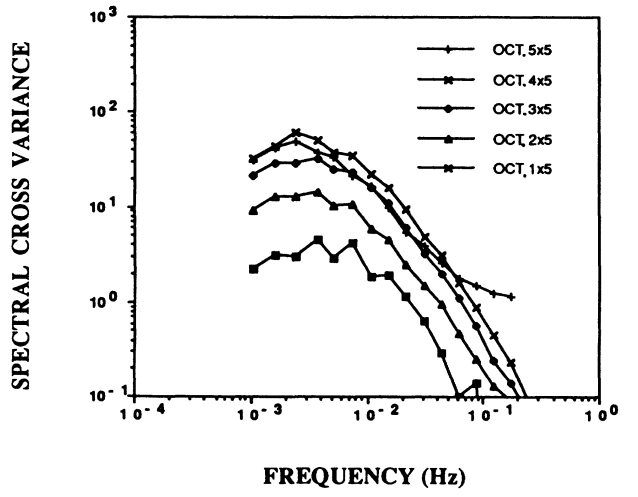

FIG. 23. Some second cross spectra are shown for the data used in Figs. 21 and 22.

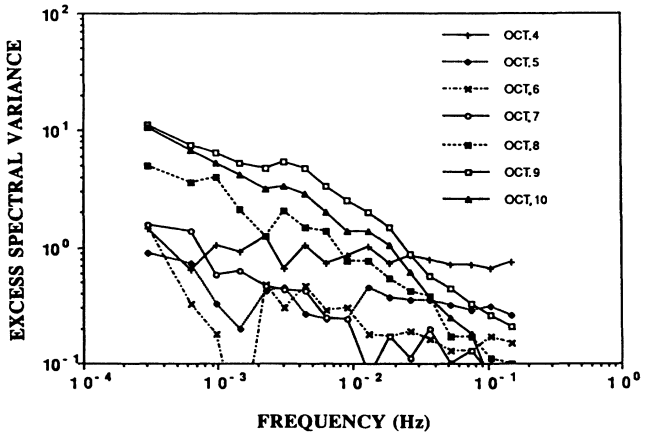

FIG. 24. Second spectra from C-Cu No. 3 at 8.3 K with a sampling rate of 852 Hz are shown.

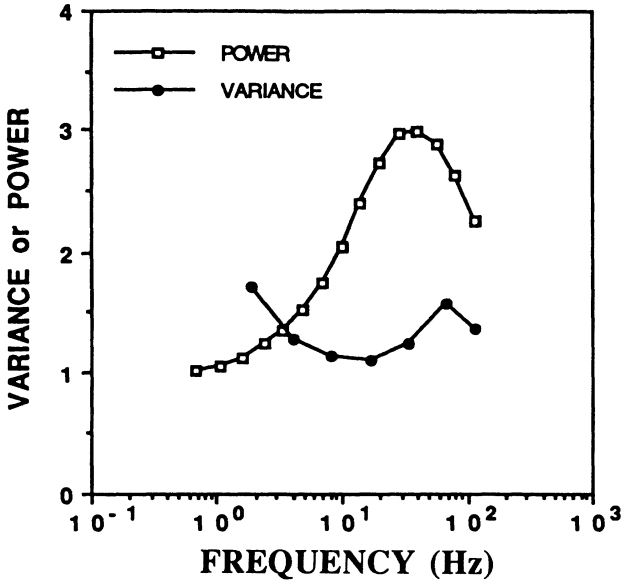

FIG. 25. The first spectrum and variance for the data used in Fig. 24 are shown.

current density near other TLS's in neighboring phase coherent regions. Unlike the other samples C-Cu No. 3 (Figs. 24 and 25) was, in fact, close to the metal-insulator transition, and so the occurrence of such modulation effects cannot in general be precluded. It should be noted that the occurrence of different frequency dependencies for second spectra in the same data set would not be expected if the noise had an extrinsic origin such as temperature or current fluctuations.

SUMMARY OF FINDINGS

In summary, the spectral features and discrete switching seen in nanometer-scale wires comprise the first observation of individual fluctuators in amorphous conductors in the metallic regime. The fluctuator density of about 1×10^{16}/K-octave cm^3 agrees well with the typical time-dependent heat capacity of amorphous materials.[2] The features observed in the noise measurements exhibited both thermally activated and tunneling behavior, as had been expected. One of the observed features showed thermally activated behavior near 10 K, with an activation energy of 15 meV, and in another case the data indicated a crossover from a weak to a strong T-dependent regime. Other features, including one at 30 K, were found to have weak T dependence consistent with tunneling kinetics. Distinguishable discrete switching, observed in most samples studied, was found to occur between two conductance levels except in one case in which the conductance switching occurred between three levels.

Several statistical parameters, in particular the second spectra, were used to quantify aspects of the fluctuations for which a simple TLS picture would give known results. Anomalous effects were usually evident in the second spectra, as long as the noise contained measurable levels of excess variance. These effects took the form of low-frequency modulations in the power of higher-frequency noise components, implying that the low-frequency fluctuator kinetics cannot be completely described by models employing independently fluctuating two-level objects. During one run, discrete switching of the power was visible in the power-time series, or second-order sweeps, and in another instance the low-frequency modulations were found to be associated with fluctuations in the duty cycle. Finally, direct evidence of non-TLS behavior was seen in some of the voltage traces exhibiting switching, though unlike the anomalies seen in the second spectra it is not clear how common such occurrences are.

The utility of noise measurements as a probe of the low-temperature properties of amorphous materials has been demonstrated. The combination of characteristic rates and temperatures that we have studied are not easily accessed by the other standard techniques. Relatively convenient techniques requiring only conventional photolithography equipment have been developed for the fabrication of suitable nanometer-scale samples. The statistical parameters employed in this work, in particular, the second spectra, have proved useful in quantifying aspects of the excitations not accessible by ordinary spectral analysis.

DISCUSSION

The electron densities in the Si-Au and C-Cu systems studied were sufficiently low that one expected the fluctuator kinetics in these systems to be similar to those of the well-studied amorphous insulators, at least for $T > 1$ K where phonon mediated interactions should dominate.[2] Several groups have observed discrete conductance jumps in semiconductor nanostructures,[8,15] including ones with amorphous junctions, and in devices containing oxide tunnel junctions. In these systems the noise and the switching are dominated by processes involving charge trapping. Such fluctuations are a small subset of the modes contributing to the heat capacity and are sensitive to Coulomb interaction effects. Thus, it is not clear *a priori* that their behavior would be similar to that of the most numerous slow modes. Likewise, the conductance steps found in metallic systems[8,14,16] do not generally reflect the behavior of amorphous materials. In the most nearly amorphous metal studied, it is not known whether the density of fluctuators was close to the expectation from the standard heat-capacity anomaly.[16] While it is not certain that the modes observed in the current experiments are qualitatively the same as those which dominate the thermal properties at slightly lower temperatures, both the density found and the expectations for universal conductance fluctuation noise indicate that we are observing atomic motions in a nonspecific way. We caution, however, that without direct measurements of time-dependent heat capacity coupled with more accurate noise measurements of the density of states on similarly prepared films, the possibility remains that the noise is dominated by a set of fluctuations which involve atypically large atomic rearrangements.

That the noise was usually Gaussian when the spectral density was featureless, and that the features, when

present, were usually stable, implies that significant structural rearrangements are not prevalent on the time scales of the measurements. In fact, the size of the features and their temperature dependences, over the range for which those dependences were reversible, were in very nice agreement with the extrapolated behavior of a conventional TLS picture. In most cases, the largest component of the non-Gaussian spectral variance was also consistent with such a picture.

On the other hand, second-order traces like those shown in Fig. 18, which appear to be more the rule than the exception, indicate clearly that deviations from independent-TLS behavior occur and are probably common. The deviations from TLS behavior indicate interactions with something slow. Since universal conductance fluctuation theory would predict that essentially all atomic motions show up in the noise, and since the approximate number of fluctuators found agrees reasonably with expectations from thermal measurements on amorphous materials, the obvious interpretation of the slow modulations in the properties of individual fluctuators is that they are due to interactions with fluctuators of the same general type. The low-frequency modulations are consistent with the general notion of strong strain mediated interactions.[7,21]

As the energy splitting of one double-well system is changed by strain mediated interactions with a neighboring double-well system fluctuating at some lower frequency, the noise power will undergo low-frequency modulations. If, for example, the strain interaction predominantly affected the energy asymmetry ΔE and not the barrier height, then we would expect modulations in the duty cycle and not the characteristic frequency. The second spectra would be identical to that expected for a three-level system in which one of the states had a much larger lifetime than the other two. In this case, Lorentzian-like features would be seen in the second spectra, as in Fig. 22. Featureless second spectra, such as $1/f$, could not easily be accounted for in this type of model, since the $1/r^3$ range of the strain interactions should limit the number of pairwise interactions for a given TLS.

There may be some problem in quantitatively accounting for the strength of the interactions observed, given that the dimensionless parameter characterizing the strain interaction strength[7] in a standard TLS picture is about 10^{-2}. However, we believe that this problem will be best dealt with by theorists.

Apart from characterizing other systems, future work in this area should address several specific issues. Is the noise below the plateau regime any different, in particular, do the interaction effects change? Are non-white-noise second spectra as common in other systems as they were found to be in the samples studied here? It would be useful to know the typical frequency dependence of second spectra to ascertain, for example, whether the fluctuators often have a few-levels character. This will require data on a larger ensemble of features, possibly over a larger frequency range. If models for interacting TLS are developed further, it may be possible to tailor other statistical measures to test them specifically. Better limits on the magnitude of the conductance jumps could provide clues to the size of the defects or clusters involved in the excitations. It may be possible to perform heat-capacity and thermal conductivity measurements on the same type of films as those used in noise studies, allowing a more quantitative analysis of the data and a more reliable connection between the noise characterization and the thermally important modes. Finally, we note that some of the techniques developed in this study may be useful for other applications; non-Gaussian effects in small-volume samples of spin glasses may discriminate between several proposed spin-glass models.

ACKNOWLEDGMENTS

Two of us, G.A.G. and M.B.W., were supported by National Science Foundation Grant No. DMR-86-17941, and G.B.A. was supported by NSF Grant No. DMR-86-12860 through the University of Illinois Materials Research Laboratory.

APPENDIX A

Here we discuss how to calculate the density of two-state systems from the variations in the spectral shape. First, we show how to calculate the variation in the spectral shape from the fluctuator density, then use simple Bayesian ideas to invert the procedure.

The random variance in $P(\omega)$ (henceforth called P without ambiguity) is easier to calculate analytically than is the random variance in γ. However, the former quantity is more likely to be affected by systematic differences between samples or by systematic annealing effects. We proceed to calculate the former quantity, and then use the very convenient simplifying assumption that the standard deviation of γ is much less than one to calculate the latter. First, we calculate the variance in P for a collection of equally large Lorentzians as a function of their density in log of characteristic frequency. Then we consider the effects of allowing a distribution of amplitudes corresponding to a flat distribution of level spacings to obtain a spectral variance as a function of density in energy-log frequency space. Then we calculate a correction to allow a distribution of amplitudes from the random effects of any atomic motions on the universal conductance fluctuation term. Finally, we show how to convert the fractional spectral density variance into a spectral slope variance on the assumption that neither is too large.

Consider the power spectrum from a finite number of fluctuators for which the logarithm of the rates τ^{-1} is uniformly distributed between the logarithms of τ_-^{-1} and τ_+^{-1}, and for which the amplitudes are also distributed about some mean. Such a spectrum will show deviations from pure $1/f$. We wish to find the magnitude of the fluctuations about the broad-band average as a function of the density of fluctuators. Let $P(\omega)=\sum_i S(\omega,\tau_i)$, where

$$S(\omega,\tau_i)=\tau_i/(1+\tau_i^2\omega^2)$$

is the Lorentzian of the ith fluctuator. If we assume the Lorentzians all have the same amplitude, the fractional

variance, or bumpiness, of $P(\omega)$ can be defined

$$\langle(\omega\,\delta P)^2\rangle/\langle\omega P\rangle^2=\langle(\omega\,\delta S)^2\rangle/N\langle\omega S\rangle^2 .$$

The quantities ωP and ωS are proportional to the octave sum of the power at ω. N is the total number of fluctuators in the interval $\{\tau_-,\tau_+\}$ and $w\,\delta P \equiv[\omega P(\omega)-\langle\omega P\rangle]$, where $\langle\omega P\rangle$ ln2 is the power per octave averaged over all octaves. Since only the product $\omega\tau$ enters the terms containing $S(\omega,\tau)$, the averages $\langle\ \rangle$ on the right-hand side represent averages over $\omega\tau$. When evaluating $\langle\ \rangle$ as a function of frequency, it is obviously important that all octaves be weighed equally, as opposed to equal weighting per unit frequency window. It is easiest, thus, to interpret $\langle\ \rangle$ as an average over all τ with ω held fixed. We must impose $\tau_+^{-1}\ll\omega\ll\tau_-^{-1}$ and $0<\tau_\pm<\infty$ in order to avoid divergences. Evaluating the averages for S we get

$$\langle(\omega S)^2\rangle\equiv[\ln(\tau_+/\tau_-)]^{-1}\int(\omega S)^2 d\tau/\tau$$
$$=\tfrac{1}{2}[\ln(\tau_+/\tau_-)]^{-1} ,$$
$$\langle\omega S\rangle\equiv[\ln(\tau_+/\tau_-)]^{-1}\int(\omega S)d\tau/\tau$$
$$=(\pi/2)[\ln(\tau_+/\tau_-)]^{-1} .$$

The fractional variance for one fluctuator in the window $\{\tau_-,\tau_+\}$ is well defined even though the quantity is much greater than unity

$$[\langle(\omega S)^2\rangle-\langle\omega S\rangle^2]/\langle\omega S\rangle^2\approx\langle(\omega S)^2\rangle/\langle\omega S\rangle^2$$
$$=(2/\pi^2)\ln(\tau_+/\tau_-) .$$

In terms of the average number of Lorentzians n' per factor of e in τ we have $N=n'\ln(\tau_+/\tau_-)$ and thus

$$\langle(\omega\,\delta P)^2\rangle/\langle(\omega P)^2\approx\langle\omega S)^2\rangle/N\langle\omega S\rangle^2=2/n'\pi^2 . \quad \text{(A1)}$$

Now suppose that the Lorentzian amplitudes are distributed as well as the characteristic times, and that the distributions are uncorrelated. In general, for any function $f(x,y)=g(x)h(y)$ with separable distributions ρ_x and ρ_y for x and for y

$$\langle f^z\rangle=\int\int g^z h^z\rho_x\rho_y\,dx\,dy=\langle g^z\rangle\langle h^z\rangle$$

and so

$$\langle f^2\rangle/\langle f\rangle^2=(\langle g^2\rangle/\langle g\rangle^2)(\langle h^2\rangle/\langle h\rangle^2) . \quad \text{(A2)}$$

The contributions to the variance are separable in this case, and the fractional fluctuations due to the amplitude spread can be computed apart from the τ spread.

Of interest is the amplitude distribution for a double-well system with a spread of energy splittings E mostly due to a spread of well asymmetries ΔE. If the characteristic high-state and low-state lifetimes are τ_u and τ_d, and $\tau_u/\tau_d=e^{-E/kT}$, and if the spectrum is $S=A\tau/(1+\tau^2\omega^2)$, then the amplitude factor A is proportional to

$$\tau_u\tau_d/(\tau_u+\tau_d)^2\sim\mathrm{sech}^2(E/2kT) .$$

Assuming a uniform distribution for E over $\{0,E_+\}$, the relevant averages are

$$\langle A\rangle=(1/E_+)\int\mathrm{sech}^2(E/2kT)dE\approx 2kT/E_+ ,$$
$$\langle A^2\rangle=(1/E_+)\int\mathrm{sech}^4(E/2kT)dE\approx\tfrac{4}{3}kT/E_+ ,$$

and the fractional variance for one fluctuator occurring with uniform probability in $\{0,E_+\}$ is

$$\langle(\delta A)^2\rangle/\langle A\rangle^2\approx\langle A^2\rangle/\langle A\rangle^2=E_+/6kT$$

(for one Lorentzian). If, instead of one fluctuator in E_+, there are q fluctuators per kT spread in E, then the total number of fluctuators in $N=qE_+/kT$, and the total fractional variance due to the amplitude spread is

$$\langle(\delta A)^2\rangle/\langle A\rangle^2\approx(1/N)E_+/6kT=1/6q . \quad \text{(A3)}$$

A density of $q=1$ corresponds to one fluctuator per factor of e in τ_u/τ_d, or equivalently per kT in level splitting. Combining the equations above, and defining $n_0\equiv n'q$, the total fractional variance due to a finite density of Lorentzians distributed in both duty cycle and rate is

$$\langle(\omega\,\delta P)^2\rangle/\langle\omega P\rangle^2=1/3\pi^2 n_0 . \quad \text{(A4)}$$

The term n_0 represents the density of Lorentzians per factor of e in rate, per factor of e in duty cycle. Equations (A1) and (A4) have been confirmed in simulations.

We may now consider the effect of having a spread in the size of the Lorentzian contributions not due to a spread in duty cycles but rather due to the random effects on the conductance of any particular motion of a few scatterers. We again use the factorizability of the moments of independent distributions, assuming that this amplitude distribution is independent of the frequency and duty-cycle distributions. The most plausible approximation is that, since universal conductance fluctuation effects arise from the sum of many weakly correlated interference terms, localized two-state systems would give rise to a Gaussian distribution for the effects of the switching on the conductance. The magnitude of the Lorentzian contributions goes as the square of that effect. Thus, the fractional variance in the spectral density, for a given concentration of fluctuating sites, will be enhanced by the ratio of the fourth moment to the square of the second moment of the Gaussian distribution, which is a factor of 3, giving

$$\langle(\omega\,\delta P)^2\rangle/\langle\omega P\rangle^2=1/\pi^2 n . \quad \text{(A5)}$$

Here n is the total density of states per factor of e in frequency per kT in energy, as would appear in the time-dependent heat capacity.

So long as the fractional variance in the spectral density is small, the variance in γ can be computed from the random slope contributed to ωP by each Lorentzian. When the Lorentzians are sparse, variations in the denominator in the logarithmic slope become important, making a problem which we could solve by simulation but not analytically. In the large n limit to convert the variance in spectral density to a variance in spectral slope, we need only to compute the ratio of the contribution of a single Lorentzian to the second moment of the derivative of P with respect to $\ln\omega$ to its contribution to the second moment of the spectral density. The result is

$$\langle(\delta\gamma)^2\rangle \approx [\langle(\omega\,\delta P)^2\rangle/\langle\omega P\rangle^2]\int \exp(2z)/(1+\exp 2z)^4 dz \Big/ \int \exp(2z)/(1+\exp 2z)^4\,dz$$
$$= [\langle(\omega\,\delta P)^2\rangle/\langle\omega P\rangle^2]/3 \ .$$

The results of simulations agree closely with this result when $\langle(\delta\gamma)^2\rangle$ is less than 0.1. Under the assumptions used above, the net result is

$$\langle(\delta\gamma)^2\rangle = 1/3\pi^2 n \ . \tag{A6}$$

Since the statistical errors in estimating the true variance in the spectral slope from a small number of independent samples are large, some care is required in handling the statistics. In particular, it is not appropriate simply to assume that the range of true variances consistent with the observed variance is given by the range of observed variances that would be found in multiple experiments on a sample whose true variances were equal to the observed value. The problem of calculating the probability distribution for an actual parameter from a measured value, given only well-defined algorithms for the inverse problem, is, of course, a familiar one, for which Bayesian techniques are best suited. The key step is to assume a prior probability distribution for the parameter, incorporating whatever prior knowledge is available. Here we use a standard assumption—the prior likelihood of any range of fluctuator densities is simply proportional to the logarithm of that range. Such a uniform distribution of probabilities of logarithms is not normalizable, but when combined with the information from the measured value gives a well-behaved probability distribution for the unknown parameter—the fluctuator density.

Since the small variance X in the spectral slope used to calculate the fluctuator density was determined from five measurements, its distribution, given an expected variance X_0, should be approximately a four degree of freedom χ^2 distribution with conditional probability density function

$$\rho(X|X_0) = 4(X/X_0^2)\exp(-2X/X_0) \ .$$

With our unbiased prior assumption concerning $\log X_0$, we find

$$\rho(X_0|X) = 4(X^2/X_0^3)\exp(-2X/X_0) \ .$$

Of more direct interest is the probability density function for the variable proportional to the fluctuator density $(1/X_0)\equiv Y_0$. Our prior assumption of a uniform logarithmic density function for X_0 is, of course, equivalent to the same assumption for Y_0:

$$\rho(Y_0|X) = 4X^2\,Y\exp(-2XY) \ ,$$

by simple change of variables. Then $\langle Y_0\rangle = 1/X$, as one might naively guess, but $Y_0 = 1/2X$ is the peak of the probability density function for Y_0. Integrating ρ gives the probability distribution function for Y_0,

$$1-(1+2XY_0)\exp(-2XY_0) \ .$$

The confidence limits are then simply obtained by numerically evaluating this probability distribution function. There is a 10% chance each for $Y_0 > 1.9/X$ or $Y_0 < 0.27/X$, giving an estimate of $Y_0 = 0.72/X$ $(\times 2.7^{\pm 1})$ with 80% confidence, where we have, for simplicity, chosen the geometric mean of the confidence limits as the estimate. Similarly, $Y_0 = 0.67/X\,(\times 3.7^{\pm 1})$ with 90% confidence.

APPENDIX B

We briefly review the statistical techniques for analyzing non-Gaussian effects in the time series here. Detailed discussions of the additional points may be found elsewhere.[18,22]

The covariance matrix, the associated second spectrum, and other statistical parameters are defined. Let P_i be the power in frequency bin i resulting from the discrete Fourier transform of a noise signal. Repeated samplings of the power P_k give an ensemble or distribution $\rho(P_k)$ that characterizes the noise. If the noise is Gaussian then the real and imaginary components of the discrete Fourier transform will have Gaussian distributions. Then it can be shown that the distribution

$$\rho(P) = \exp[-P/\langle P\rangle]/\langle P\rangle$$

for which the variance $\langle(\delta P)^2\rangle = \langle P\rangle^2$, where $\langle P\rangle$ is the mean power. Instead of studying P_i, we usually study the octave sum $O_i = \sum_k P_k$ where the sum extends over all bins k in octave i. In this case the variance $\langle\delta O_i^2\rangle = \sum_k \langle P_k\rangle^2$. If the spectrum is white noise then the distribution $\rho(O_j)$ can be seen to be a $2m_i$ degree of freedom chi-squared distribution where m_i is the number of bins in octave i, and the variance becomes $\sum_k \langle P_k\rangle^2 = \langle O_i\rangle^2/m_i$. We define the normalized covariance matrix c_{ij} by

$$c_{ii} = \langle\delta O_i^2\rangle \Big/ \sum_k \langle P_k\rangle^2 \ ,$$

where the summation extends over all bins k in octave i and, for $i \neq j$,

$$c_{ij} = \langle\delta O_i\,\delta O_j\rangle/(\langle\delta O_i^2\rangle\langle\delta O_j^2\rangle)^{-1/2} \ .$$

If the noise is Gaussian then $\langle c_{ii}\rangle = 1$, and since fluctuations in distinct bins are uncorrelated then $\langle c_{i\neq j}\rangle = 0$. For a given sampling rate a spectrum can be conveniently divided into approximately seven well-defined octaves, so the covariance matrix indices (i,j) extend from 1–7.

As a simple example consider a 5% duty-cycle two-level switcher ($\tau_{\min}/\tau_{\max} = \frac{1}{19}$, where τ refers to the average lifetimes for each of the two states of the TLS) with characteristic frequency f_0, in the presence of a $1/f$ Gaussian background signal. The variance c_1 for this signal is given in Fig. 26 for the case of a switcher to background power ratio of 1, evaluated at f_0. At high and low octaves the background dominates and $c \approx 1$,

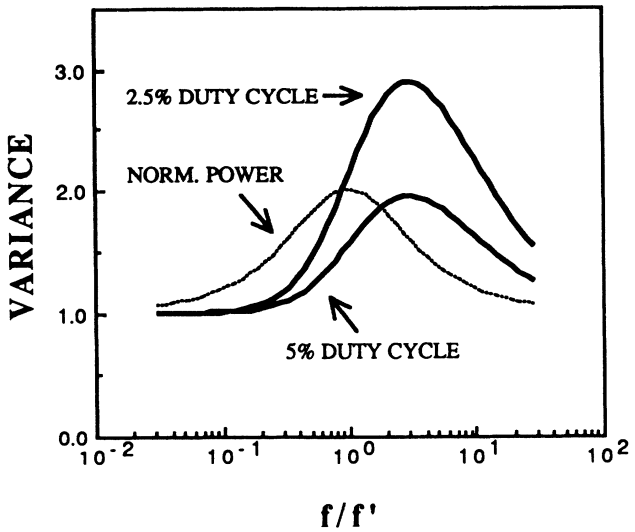

FIG. 26. The normalized variance as a function of frequency is shown for a two-state random telegraph in the presence of a $1/f$ Gaussian background. Two duty cycles are illustrated.

while in octaves near f_0 the signal variance significantly exceeds the Gaussian prediction. In the low-duty-cycle limit the switcher signal can be thought of as a series of pulses, and the increased power variance results from the increased fractional variance $\langle(\delta m)^2\rangle/\langle m\rangle^2$ in the number of pulses (m) occuring per sweep. As the duty cycle decreases at fixed power values the variance

$$c_i \approx \langle(\delta m)^2\rangle/\langle m\rangle^2 \approx (\tau_{\min}/\tau_{\max})^{-1}$$

will increase. Analytic expressions for c_i which can easily be evaluated for the low-duty-cycle limit are in agreement with simulations.[18,22] Simulations of the high-duty-cycle limit ($\tau_{\min}/\tau_{\max}\approx 1$) lead to variance spectra which are slightly lower in magnitude and which peak about one to two octaves above the equivalent low-duty-cycle peak.[12] If the background is Gaussian, the excess variance $c_i - 1$ scales as the square of the ratio of the spectral density of the non-Gaussian component to the total spectral density. For all signal-to-background ratios and arbitrary duty cycle, c_i is always found to peak at least one and one half to two octaves above the peak in the power, and the peak octave will move to arbitrarily high frequencies as the signal-to-background ratio increases. Given the spectral density O_i, the variance c_i, and the background, one can uniquely determine the amplitude and duty cycle of a two-state switcher. In practice, uncertainty in the background limits the accuracy of the prediction.

Other systems which have been modeled include particles diffusing in a $1-d$ random potential,[12] and a facilitated kinetic Ising model.[23] Unlike the two-level switchers, however, these systems generally exhibit variances which increase monotonically with octave number and which are sampling rate dependent. This behavior results whenever the fractional fluctuations $\langle\delta O_i^2\rangle/\langle O_i\rangle^2$ are roughly comparable in magnitude for all i, and can be expected for many systems which incorporate strong interactions. These systems are also characterized by fluctuations in noise power in some frequency band which are slow compared with the characteristic frequency of the band itself, which suggests that a more complete description of the time course of the power fluctuations should be useful.

The "second spectrum" represents such a description of the kinetics of the fluctuations in noise power. The second spectrum of octave i is defined as the absolute square of the fast Fourier transform $\mathcal{F}$ of power samplings O_i; letting R denoted the second spectrum, we have $R_{ii}=|\mathcal{F}[O_i]|^2$. This is defined in exact analogy with the usual spectral density, except with the voltage samplings $\{V(t=0),V(1),\ldots,V(1023)\}$ replaced with the power samplings $\{0_i(0),0_i(1),\ldots,O_i(1023)\}$. To avoid confusion, we refer to the power samplings $\{O_i\}$ as the "second-order sweep." Since each second-order sweep requires $(1024)^2$ voltage samplings, practical considerations limit the number of second-order sweeps that can be acquired. Second-order cross spectra can also be defined [i.e., $R_{ij}=\mathrm{Re}(\mathcal{F}[O_i]\times\mathcal{F}^*[O_i])$], the variance c_{ii} can be expressed in terms of the second spectrum as

$$\sum_{k\neq 0}[R_{ii}(\omega_k)]=\langle(\delta O_i)^2\rangle=c_{ii}\sum P_k^2$$

(where the first sum extends over all frequency bins except $\omega=0$). A similar equation applies for the off-diagonal terms. Hence, there is a spectrum describing the frequency decomposition of each element of the covariance matrix.

The central result used here concerns the shape of the second spectrum for two-state Markov systems. Such a system is fully characterized by two characteristic rates for switching between the two states.[24] The fluctuations are dominated by high-duty-cycle fluctuators, which have approximately equal values for these two rates. These, then, have no characteristic frequencies much below the peak in the ordinary spectrum. Since the highest usable octave in the second spectrum is about a decade below the lowest usable octave in the ordinary spectrum, and nearly three decades below the highest octaves, from which most of our second spectrum data are taken, high-duty-cycle two-state fluctuators cannot give significantly non-white-noise second spectra. For extremely low-duty-cycle two-state fluctuators, with much less than one pulse, on the average, per sweep, the likelihood of a pulse in any sweep is independent of what happened in previous sweeps, again giving a white-noise second spectrum. Only two-state systems with characteristic frequencies near or below the lower end of the first spectrum can give slightly non-white-noise second spectra, observable mainly in the lowest octaves of the first spectrum. Strong frequency dependence in the second spectrum can be expected in systems involving interacting fluctuators.[23] In the C-Cu and Si-Au we observed non-white-noise second spectra mainly in the higher octaves of the first spectrum, in the absence of any indications of tails of large low-frequency contributions to the first spectrum, and with characteristic frequencies usually extending to less than the lowest frequency observed in the second spectrum. Thus, this behavior bears no resemblance to the second spectra obtainable from two-state systems.

*Current address: IBM, East 16/014, 5600 Cottle Rd., San Jose, CA 95193.

[1]R. C. Zeller and R. O. Pohl, Phys. Rev. B **4**, 2029 (1971).

[2]W. A. Phillips, Rep. Prog. Phys. **50**, 1657 (1987).

[3]For example, S. Grondey, H. V. Lohneysen, H. J. Schink, and K. Samwer, Z. Phys. B **51**, 287 (1983).

[4]P. W. Anderson, B. I. Halperin, and C. Varma, Philos. Mag. **25**, 1 (1972); W. A. Phillips, J. Low Temp. Phys. **7**, 351 (1972).

[5]U. Buchenau, H. M. Zhou, N. Nicker, K. Gilroy, and W. A. Phillips, Phys. Rev. Lett. **60**, 1318 (1988).

[6]E. R. Grannan, M. Randeria, and J. P. Sethna, Phys. Rev. Lett. **60**, 1402 (1988).

[7]C. Yu and A. J. Leggett, Comments Cond. Matter Phys. **14**, 231 (1988).

[8]M. B. Weissman, Rev. Mod. Phys. **60**, 537 (1988), and extensive references therein.

[9]S. Feng, P. A. Lee, and A. D. Stone, Phys. Rev. Lett. **56**, 1960, 2772 (1986); P. A. Lee, A. D. Stone, and H. Fukuyama, Phys. Rev. B **35**, 1039 (1987).

[10]G. A. Garfunkel, G. B. Alers, M. B. Weissman, J. M. Mochel, and D. J. van Harlingen, Phys. Rev. Lett. **60**, 2773 (1988); N. O. Birge, B. Golding, and W. H. Haemmerle, *ibid.* **62**, 195 (1989).

[11]M. Nelkin and A.-M. S. Tremblay, J. Stat. Phys. **25**, 253 (1981).

[12]P. J. Restle, R. J. Hamilton, M. B. Weissman, and M. S. Love, Phys. Rev. B **31**, 2254 (1985).

[13]P. J. Restle, M. B. Weissman, and R. D. Black, J. Appl. Phys. **54**, 5844 (1983).

[14]K. S. Ralls and R. A. Buhrman, Phys. Rev. Lett. **60**, 2434 (1988).

[15]M. J. Kirton and M. J. Uren, Adv. Phys. **38**, 367 (1989), and extensive references therein; also, e.g., K. R. Farmer, C. T. Rogers, and R. A. Buhrman, Phys. Rev. Lett. **56**, 1960 (1987); R. T. Wakai and D. J. VanHarlingen, *ibid.* **58**, 1687 (1987).

[16]D. E. Beutler, T. L. Meisenheimer, and N. Giordano, Phys. Rev. Lett. **58**, 1240, 2608 (1987); for a review of similar experiments in metallic samples see, N. Giordano, in *Mesoscopic Physics,* edited by B. L. Al'tshuler, P. A. Lee, and R. A. Webb (North-Holland, Amsterdam, in press).

[17]G. A. Garfunkel, G. B. Alers, M. B. Weissman, and N. E. Israeloff, Phys. Rev. B **40**, 8049 (1989).

[18]G. A. Garfunkel, Ph. D. Dissertation, University of Illinois, 1989; and (unpublished).

[19]D. E. Prober, M. D. Feuer, and N. Giordano, Appl. Phys. Lett. **37**, 94 (1980).

[20]J. Jackle, Z. Phys. **257**, 212 (1972).

[21]M. W. Klein, B. Fischer, A. C. Anderson, and P. J. Anthony, Phys. Rev. B **18**, 5887 (1978).

[22]P. J. Restle, Ph. D. Dissertation, University of Illinois, 1985.

[23]G. B. Alers, M. B. Weissman, A. Kinzig, and N. E. Israeloff, Phys. Rev. B **36**, 8429 (1987).

[24]S. Machlup, J. Appl. Phys. **25**, 341 (1954).